5990 J. Med. Chem. 2009, 52, 5990–5998
DOI: 10.1021/jm900641r

Journal of Medicinal Chemistry Article

Carbonic Anhydrase Inhibitors. Comparison of Aliphatic Sulfamate/Bis-sulfamate Adducts with Isozymes II and IX as a Platform for Designing Tight-Binding, More Isoform-Selective Inhibitors†

Rosa Maria Vitale,‡,# Vincenzo Alterio,§,# Alessio Innocenti,∥ Jean-Yves Winum,⊥ Simona Maria Monti,§ Giuseppina De Simone,*,§ and Claudiu T. Supuran*,§

‡*Istituto di Chimica Biomolecolare—CNR, Via Campi Flegrei 34, 80078, Pozzuoli, Italy,* §*Istituto di Biostrutture e Bioimmagini—CNR, Via Mezzocannone 16, 80134 Napoli, Italy,* ∥*Laboratorio di Chimica Bioinorganica, Università degli Studi di Firenze, Rm. 188, Via della Lastruccia 3, I-50019 Sesto Fiorentino, Firenze, Italy, and* ⊥*Institut des Biomolécules Max Mousseron (IBMM), UMR 5247 CNRS-UM1-UM2, Bâtiment de Recherche Max Mousseron, Ecole Nationale Supérieure de Chimie de Montpellier, 8 Rue de l'Ecole Normale, 34296 Montpellier Cedex, France.* # *These authors contributed equally to the paper.*

Received May 15, 2009

Two approaches were used to design inhibitors of the metalloenzyme carbonic anhydrase (CA, EC 4.2.1.1): the tail and the ring approaches. Aliphatic sulfamates constitute a class of CA inhibitors (CAIs) that cannot be classified in either one of these categories. We report here the detailed inhibition profile of four such compounds against isoforms CAs I−XIV, the first crystallographic structures of these compounds in adduct with isoform II, and molecular modeling studies for their interaction with hCA IX. Aliphatic monosulfamates/bis-sulfamates were nanomolar inhibitors of hCAs II, IX, and XII, unlike aromatic/heterocyclic sulfonamides that promiscuously inhibit most CA isozymes with low nanomolar affinity. The bis-sulfamates incorporating 8 or 10 carbon atoms showed higher affinity for the tumor-associated hCA IX compared to hCA II, whereas the opposite was true for the mono-sulfamates. The explanation for their interaction with CA active site furnishes insights for obtaining compounds with increased affinity/selectivity for various isozymes.

Introduction

A paradigm in carbonic anhydrase (CA,[a] EC 4.2.1.1) drug design was that aliphatic sulfonamides RSO_2NH_2 (R = aliphatic group) are inactive as inhibitors, unlike the aromatic/heterocyclic ones of the type $ArSO_2NH_2$.[1] This view was subsequently challenged, being shown that aliphatic sulfonamides incorporating perhaloalkyl moieties of the type $C_nX_{2n+1}SO_2NH_2$ (n = 1−4, X = F, Cl),[2] as well as various aliphatic sulfamates/bis-sulfamates[3−5] potently inhibit several CA isozymes involved in fundamental physiologic/pathologic states. Indeed, this family of metalloenzymes comprises 16 different isoforms, of which several are cytosolic (CAs I−III, CA VII, and CA XIII), five are membrane-bound (CA IV, CA IX, CA XII, CA XIV, and CA XV), two are mitochondrial (CAs VA and VB), and one (CA VI) is secreted into saliva/milk.[6−13] Three acatalytic forms are also known, i.e., CA VIII, CA X, and CA XI.[9] These enzymes are involved in crucial physiological processes connected with respiration and transport of CO_2/bicarbonate between metabolizing tissues and lungs, pH and CO_2 homeostasis, electrolyte secretion in a variety of tissues/organs, biosynthetic reactions (such as gluconeogenesis, lipogenesis, and ureagenesis), bone resorption, calcification, tumorigenicity, and several other physiologic/pathologic processes. Consequently many of them are also well-established drug targets.[6−13] In fact, sulfonamide CA inhibitors (CAIs) such as acetazolamide AAZ, methazolamide MZA, dorzolamide DZA, or brinzolamide BRZ (Chart 1), among others, are clinically used agents as diuretics[6,7] and for the management of a variety of disorders connected to CA disbalances, such as glaucoma, edema due to congestive heart failure,[7,8] or drug-induced edema.[7,8] Other agents of this pharmacological class show applications as anticonvulsants,[12] and antiobesity[13] or antitumor drugs/tumor diagnostic agents.[5,6,9,11,14]

Many classes of new CAIs are constantly being reported[15] because of at least two reasons: (i) the large number of catalytically active isoforms (12 in primates, 13 in other mammals),[6] which are drug targets for many types of applications, as mentioned above[6−14] (for example, the antiglaucoma sulfonamide drugs target CAs II, IV, and XII, the antiobesity CAIs target CA VA and CA VB, the anticonvulsant ones probably target CA VII and XIV, whereas the antitumor drugs/diagnostic agents target the transmembrane isoforms overexpressed in tumors, CAs IX and XII)[5,6,9,11,14] and (ii) the lack of isozyme selectivity of the presently available, clinically used compounds.[6]

Considering the fact that, as mentioned above, aliphatic derivatives received scant attention as CAIs[1−5] and that the adduct of hCA II with $CF_3SO_2NH_2$[2b] represented the unique complex of a linear aliphatic sulfonamide to be characterized in complex with a CA isozyme,[16] we decided to investigate in some detail aliphatic sulfamates/bis-sulfamates as a platform for designing tight-binding, possibly isoform-specific CAIs. In this paper we report on the high resolution crystallographic

† The X-ray coordinates of the hCA II−sulfamate adducts are available in the Protein Data Bank with the IDs 3IBI, 3IBU, 3IBL, 3IBN.

*To whom correspondence should be addressed. For G.D.S.: phone, +39-081-2534579; fax, +39-081-2536642; e-mail, gdesimon@unina.it. For C.T.S.: phone, +39-055-4573005; fax, +39-055-4573385; e-mail, claudiu.supuran@unifi.it.

[a] Abbreviations: CA, carbonic anhydrase; CAI, CA inhibitor; hCA, human carbonic anhydrase; mCA, murine carbonic anhydrase; MD, molecular dynamics.

 Published on Web 09/04/2009

Chart 1

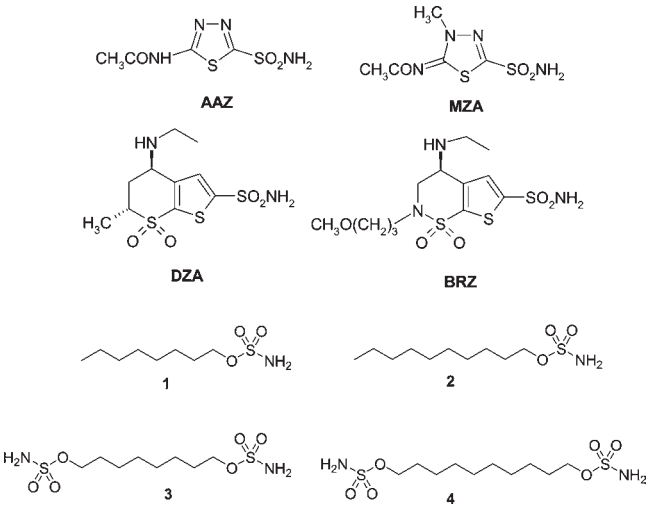

structure of sulfamates **1**−**4** in complex with the cytosolic dominant isoform hCA II, together with a molecular modeling study of the adducts of some of these CAIs with the tumor-associated isoform hCA IX, a recently validated drug target.[17] This combined approaches give a possible explanation for the experimentally observed different affinities of this class of compounds toward various isozymes (e.g., hCA II and hCA IX), providing useful insights for the design of more isozyme-selective inhibitors mainly targeting the tumor-associated CA IX.

Results and Discussion

Chemistry and CA Inhibition. Sulfamates/bis-sulfamates **1**−**4** incorporating linear aliphatic chains with 8 or 10 carbon atoms have been reported earlier by our groups[3−5] and tested for the inhibition of 3 CA isozymes of the 16 known in mammals, i.e., CAs I, II, and IX. Considering the very interesting inhibition profile observed against these isoforms,[3−5] we report here the complete inhibition profile of the four sulfamates against all the catalytically active human isozymes, CAs I−XIV (Table 1).

At this point, it is worth mentioning that two main approaches were used for the drug design of CAIs up to now: (i) the "ring" approach,[19] which led to the discovery of DZA, BRZ, and the other clinically used sulfonamides, involving exploring a great variety of ring systems on which the sulfonamide group (as a zinc-binding group [ZBG]) has been attached, and (ii) the "tail" approach,[20] consisting of attaching tails that will induce the desired physicochemical properties (e.g., water solubility, liposolubility, membrane impermeability, etc.) to different scaffolds of well-known aromatic/heterocyclic sulfonamides possessing affinity for the CA active site. It is observed that the aliphatic sulfamates investigated here in detail do not belong to any of these two categories of CAIs, constituting thus a third, less understood but general class of CAIs possessing a very simple scaffold (a linear aliphatic chain) to which one or two ZBGs are attached. Thus, the present types of derivatives bring new insights into the design of CAIs, even if they are chemically very simple entities.

Data of Table 1 show the following SAR for the inhibition of isoforms CAs I−XIV with sulfamates **1**−**4** (and AAZ or DZA as standard inhibitors, presented here for comparison):

Table 1. Inhibition Data of Sulfamates **1**−**4** and Sulfonamides AAZ and DZA against CA Isoforms hCAs I−XIV by a Stopped-Flow CO_2 Hydrase Assay[18]

	K_I (nM)[d]					
isozyme[a]	**1**	**2**	**3**	**4**	AAZ	DZA
hCA I[b]	3.7[e]	530[f]	378[g]	890[g]	250	50000
hCA II[b]	2.6[h]	0.7[f]	14.6[g]	24.5[g]	12	9
hCA III[b]	9100	877	1128	1206	200000	770000
hCA IV[b]	79.9	67.6	84.1	91.2	74	8500
hCA VA[b]	1254	805	1202	1368	63	42
hCA VB[b]	624	888	1457	1592	54	33
hCA VI[b]	795	1334	1020	1414	11	10
hCA VII[b]	76.6	88.9	79.6	92.3	2.5	3.5
hCA IX[c]	25.0[e]	23.1[f]	4.0[g]	7.0[g]	25	52
hCA XII[c]	7.0	7.9	7.9	8.2	5.7	3.5
mCA XIII[b]	1125	956	569	960	17	18
hCA XIV[b]	390	711	605	852	41	27

[a] h = human; m = murine isozyme. [b] Full length enzyme. [c] Catalytic domain. [d] Mean value from at least three different measurements.[18] Errors were in the range of ±5% of the obtained value (data not shown). [e] A value of 3.5 nM has been reported in ref 3. [f] From ref 4. [g] From ref 5. Data of AAZ and DZA are from ref 6. [h] A value of 2.7 nM has been reported in ref 3.

(i) Sulfamates **1**−**4** act as strong inhibitors of 3 of the 12 CA isozymes, i.e., CAs II, IX, and XII, with inhibition constants in the range of 0.7−25.0 nM. In addition, **1** is also a very good hCA I inhibitor (K_I of 3.5 nM), being, as far as we know, the most potent inhibitor of this isoform ever reported.[6,19] It may be observed that for hCA II the monosulfamates are better inhibitors than the bis-sulfamates. For the two monosulfamates **1** and **2** (against hCA II) derivative **2** is 3.8 times a better inhibitor than derivative **1**, whereas for the bis-sufamates **3** and **4**, the shorter derivative **3** is a more effective inhibitor compared to the longer one **4**. For the inhibition of hCA IX the bis-sulfamates **3** and **4** were more effective inhibitors compared to the monosulfamates **1** and **2**, whereas against hCA XII all four derivatives showed very similar inhibitory properties, with inhibition constants only ranging between 7.0 and 8.2 nM (Table 1). Two clinically used drugs AAZ and DZA show rather comparable inhibitory activity with sulfamates **1**−**4** against these three isozymes.

(ii) Sulfamates **1**−**4** also effectively inhibited isoforms hCA IV and hCA VII, with inhibition constants of < 100 nM, i.e., in the range of 67.6−92.3 nM (Table 1). The monosulfamates **1** and **2** were slightly more effective inhibitors than the corresponding bis-sulfamates **3** and **4** against both isoforms, whereas the length of the aliphatic chain variably affected activity. In particular, for hCA IV and the monosulfamates, the best activity was observed for derivative **2**, whereas for the bis-sulfamates the best activity was observed for derivative **3**. For hCA VII, the monosulfamate and bis-sulfamate **1** and **3** were more active than longer derivatives **2** and **4**. The two clinically used drugs on the other hand behave as potent hCA VII inhibitors; AAZ was a medium potency hCA IV inhibitor, whereas DZA was a weak hCA IV inhibitor (Table 1).

(iii) The remaining seven CA isoforms, i.e., CAs I, III, VA, VB, VI, XIII, and XIV, were weakly inhibited by sulfamates **1**−**4** (except **1** which, as shown above, was a very potent hCA I inhibitor), with inhibition constants in the range of 378−9100 nM (Table 1). Several important questions remain unanswered: Why is **1** such a potent hCA I inhibitor, whereas its congeners **2**−**4** are 108−254 times less effective inhibitors of this isozyme? Why are these sulfamates 85−877 times

Table 2. Crystal Parameters, Data Collection, and Refinement Statistics for the Adducts of Sulfamates **1**−**4** with hCA II

	inhibitor			
	1	**2**	**3**	**4**
		Crystal Parameters		
space group	$P2_1$	$P2_1$	$P2_1$	$P2_1$
unit-cell parameters				
a (Å)	42.00	42.07	42.15	41.99
b (Å)	41.22	41.41	41.41	41.34
c (Å)	71.67	71.97	71.99	71.85
β (deg)	104.24	104.29	104.52	104.25
		Data Collection Statistics		
temperature (K)	100	100	100	100
resolution range (Å)	20.00−1.93	20.00−1.41	20−1.55	20.00−2.20
total reflections	47038	169645	122960	36037
unique reflections	17190	46508	32941	11593
completeness (%)	95.2 (96.5)	97.8 (78.5)	94.3 (84.2)	94.7 (85.1)
R_{sym}[a]	0.037 (0.051)	0.055 (0.199)	0.056 (0.225)	0.084 (0.240)
mean $I/\sigma(I)$	18.9 (13.9)	18.3 (5.6)	19.4 (5.0)	12.2 (4.0)
		Refinement Statistics		
resolution range (Å)	20.0−1.93	20.0−1.41	20.00−1.55	20.00−2.20
no. of reflections	17173	45982	32410	11162
R[b] (%)	16.9	20.0	17.9	18.7
R_{free}[b] (%)	20.5	21.5	20.0	22.3
rmsd from ideal geometry				
bond length (Å)	0.007	0.007	0.007	0.007
bond angle (deg)	1.4	1.4	1.5	1.5
residues	3−260	3−261	3−261	3−261
no. of protein atoms	2049	2059	2059	2059
no. of water molecules	322	363	336	171
no. of inhibitor atoms	13	15	18	20
average B factor (A^2)				
all atoms	12.5	13.9	14.0	18.4
protein atoms	11.7	11.8	12.1	17.7
inhibitor atoms	13.3	17.4	22.1	42.6
PDB accession codes	3IBI	3IBU	3IBL	3IBN

[a] $R_{sym} = \sum_{hkl}\sum_i |I_i(hkl) - \langle I(hkl)\rangle| / \sum_{hkl}\sum_i I_i(hkl)$, where $I_i(hkl)$ is the ith measurement and $\langle I(hkl)\rangle$ is the weighted mean of all measurements of $I(hkl)$. [b] $R = \sum_{hkl}||F_o(hkl)| - |F_c(hkl)|| / \sum_{hkl}|F_o(hkl)|$; R_{free} calculated with 5% of data withheld from refinement. Values in parentheses refer to the highest resolution shell.

better hCA III inhibitors compared to AAZ and DZA (which, as most sulfonamides/sulfamates investigated so far, act as very weak CA III inhibitors)?[21]

It is also observed that the two clinically used compounds AAZ and DZA strongly inhibit all seven of these CAs, except CA III, as mentioned above, with K_I values in the range of 2.5−52 nM. Consequently, the aliphatic sulfamates show a much more isoform-selective inhibition profile compared to the aromatic/heterocyclic sulfonamides in clinical use, as at least six isoforms that are potently inhibited by sulfonamides are not inhibited significantly by this class of CAIs.

Crystallography. To determine the key interactions and molecular features that contribute to high inhibitory properties of aliphatic sulfamates **1**−**4** toward hCA II, these compounds have been cocrystallized with this isozyme. Crystals of the hCA II/inhibitor adducts were isomorphous with those of the native protein,[22] allowing for the analysis of the three-dimensional structures by difference Fourier techniques. Data collection and refinement statistics for each complex structure are shown in Table 2.

Inhibitor binding did not generate major hCA II structural changes in any of the enzyme−inhibitor complexes studied; in fact, the rmsd for the superposition of the corresponding Cα atoms between the native enzyme and each enzyme−inhibitor complex ranged from 0.277 to 0.298 Å. In the active site region of each complex, a well resolved electron density, fully compatible with the inhibitor molecule, was visible (Figure 1). The binding mode of the four inhibitors to the enzyme is quite similar. In particular, the ionized sulfamate NH^- group coordinates to Zn^{2+} ion and donates a hydrogen bond to Thr199OG, while one of the two sulfamate oxygens accepts a hydrogen bond from the backbone NH group of Thr199. The aliphatic tails adopt a similar conformation (Figure 2), all of them pointing toward the hydrophobic part of the active site (the so-called "hydrophobic wall") and making numerous van der Waals interactions with residues placed in this region (Figure 1). Specifically, the aliphatic tails of the two monosulfamates **1** and **2** are almost perfectly superimposable. In the same manner, the tails of the two bis-sulfamates **3** and **4** adopt a rather similar conformation but not equal to that characterizing the monosulfamate compounds, as evidenced by the differences in torsion angles $\chi_1-\chi_4$ (see Table 3 and Figure 2).

Comparison of the structures of the four complexes reported here provides a reasonable explanation for the different affinities of the inhibitors toward hCA II (see Table 1). In particular, the elongation of the monosulfamate alkyl chain from 8 (compound **1**) to 10 (compound **2**) carbon atoms increased the inhibitory capability of the second compound, which is one of the best hCA II inhibitor

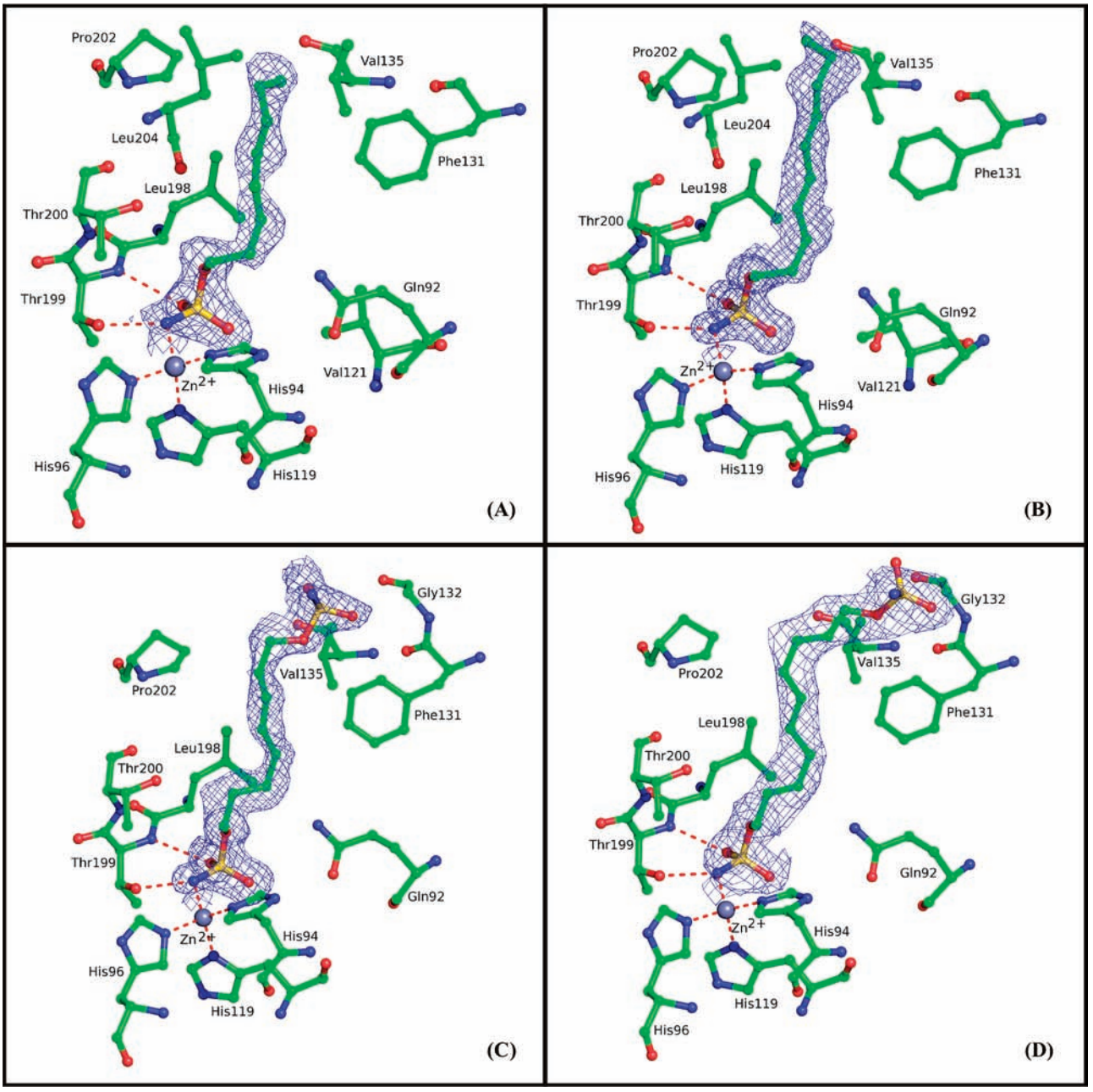

Figure 1. Active site regions in the hCA II−**1** (A), hCA II−**2** (B), hCA II−**3** (C), and hCA II−**4** complexes. Hydrogen bonds, active site Zn^{2+} coordination, and residues establishing strong van der Waals (distance of <4.5 Å) interactions with the inhibitors are also shown. The simulated annealing omit $|2F_o - F_c|$ electron density maps relative to the inhibitor molecules are reported.

Table 3. Torsion Angles (deg) of the Aliphatic Tail of Compounds **1**−**4**

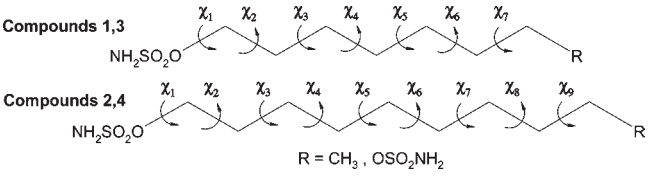

	χ_1	χ_2	χ_3	χ_4	χ_5	χ_6	χ_7	χ_8	χ_9
1	109	65	86	−165	−156	165	−61		
2	106	60	75	−179	177	−177	171	163	90
3	175	−69	−173	−70	168	168	−166		
4	174	−64	−178	−65	177	173	−173	65	−162

reported in the literature.[6,16] This phenomenon can be ascribed to the increase of the contact area between the tail and the hydrophobic wall of the enzyme active site, which improved the binding of the inhibitor. In contrast, the elongation of the bis-sulfamate alkyl chain from 8 (compound **3**) to 10 (compound **4**) carbon atoms reduced the inhibitory activity. In fact, in this case the presence of the second sulfamate group makes the tail longer than the depth of the catalytic cleft (∼15 Å),[23] thus forcing the polar extremity of the tail to bend upon the helix incorporating residues Asp130-Val135. However, because of the hydrophobic character of the helix, this second sulfamate moiety cannot establish polar interactions with hCA II in the complex hCA II−**3** or in the complex hCA II−**4**. In conclusion in the case of bis-sulfamates **3** and **4**, the more flexible

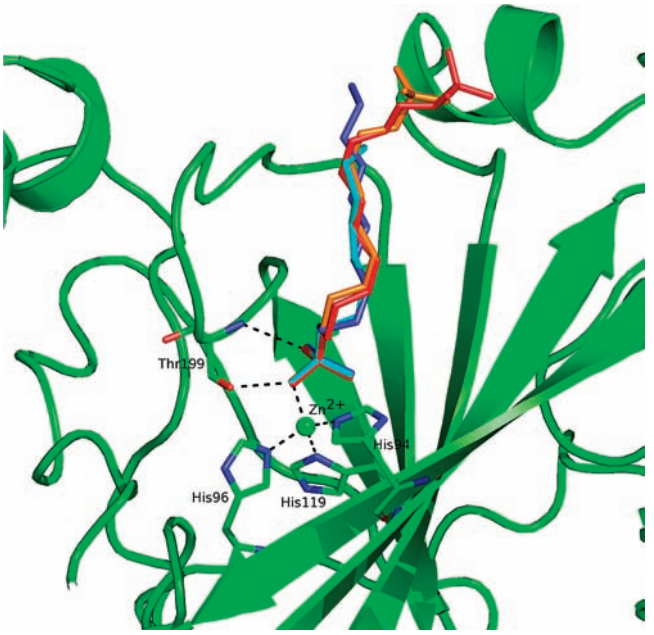

Figure 2. Superposition of hCA II−inhibitor adducts. **1** is reported in cyan, **2** in blue, **3** in orange, and **4** in red.

and polar inhibitor tail is not properly stabilized by an increased number of enzyme/inhibitor van der Waals interactions. In agreement with this finding, high *B* factors characterize the more external part of the bis-sulfamate chains, especially for compound **4** when bound to the enzyme active site (see Table 2).

Modeling Studies. To assess the molecular basis of the differences observed in the affinity of aliphatic monosulfamates and bis-sulfamates toward hCA II and hCA IX (see Table 1), the hCA IX model was built by homology modeling, following the same procedure previously described by our groups[14a] and subsequently used to manually dock compounds **2** and **4** in the enzyme active site (see Experimental Section for details). The structural comparison of hCA IX−**2** and hCA IX−**4** complexes with the corresponding adducts with hCA II revealed that the region of the hCA IX active site encompassing the short helical region defined by amino acid residues 130−136 and the loop incorporating residues 198−204 bear a number of potential critical mutations in the tumor-associated isoform (hCA IX) compared to the cytosolic one (hCA II). In particular, the hCA II residues Phe131, Gly132, and Val135 in this helical region are replaced in hCA IX by Val, Asp, and Leu, respectively, whereas residue Leu204 in the loop is mutated into Ala. To investigate the potential influence of these residues on the different affinities exhibited by inhibitors **2** and **4** toward the two isozymes, free molecular dynamic (MD) simulations of 3 ns were carried out on both hCA II−inhibitor X-ray structures and hCA IX−inhibitor theoretical models. The last 1.5 ns of all four MD simulations was used for the subsequent trajectory analysis. As shown in Figure 3, both rmsd of all heavy atoms and the atomic fluctuations relative to the Cα atoms revealed a similar behavior among the four simulations, not a trivial result considering that two of them (CA IX complexes) are derived from a modeled protein structure. In addition, well converged trends were observed for rmsd, with no hints of large scale conformational transitions.

A careful analysis of the four MD trajectories revealed that while the tetrahedral geometry of the Zn^{2+} binding site

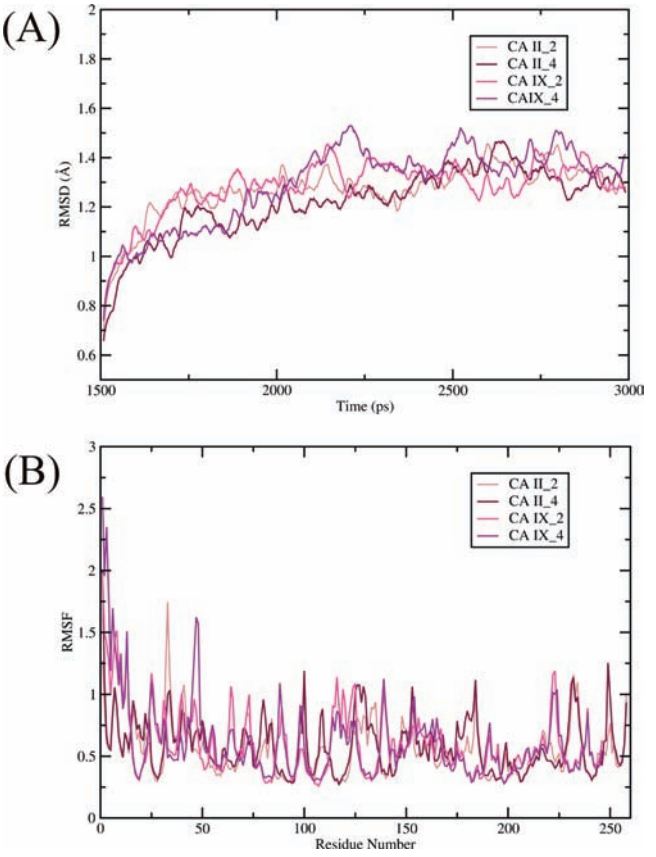

Figure 3. (A) Root mean square deviations for all heavy atoms as a function of time and (B) Cα atom root mean square fluctuations (RMSF) as a function of the residue number during the last 1.5 ns of MD simulations for the adducts of compounds **2** and **4** with hCA II and hCA IX.

and the key hydrogen bonds between the sulfamate moiety of the inhibitor and the enzyme active site were preserved in all complexes, different patterns of van der Waals and/or hydrogen bond interactions involving the active site residues and inhibitor tails could be observed. According to the X-ray structure, the analysis of the MD trajectory revealed that the hCA II−**2** complex is stabilized by a number of van der Waals interactions between the inhibitor alkyl moiety and the hydrophobic residues lying on the aforementioned helical and loop regions, which are not conserved in the corresponding hCA IX complex, thus accounting for the lower affinity of the inhibitor toward hCA IX with respect to hCA II (Figures 2 and 4A). In particular, the van der Waals interactions involving Leu204 in the hCA II complex, occurring along the entire production run, were drastically attenuated in the hCA IX adduct not only by the replacement of the Leu bulky residue with the smaller alanine but also by the concurrent mutation of Val135 into a Leu. In fact, Ala204 in hCA IX, similar to its counterpart Leu204 in hCA II, is located on the re-entrant side of the loop that exposes the Pro202 residue, forming in turn a sort of "gate" with residue Val135, located at the end of the helix. This gate is narrowed in hCA IX with respect to hCA II because of the Val/Leu mutation, thus hampering a free access to the inhibitor alkyl moiety. The mutations Phe131/Val and Gly132/Asp also play a key role in lowering the affinity of the inhibitor toward hCA IX with respect to hCA II. In fact, in the first case the shorter side chain of the valine residue weakens the van der Waals interaction with the inhibitor, while in the second one,

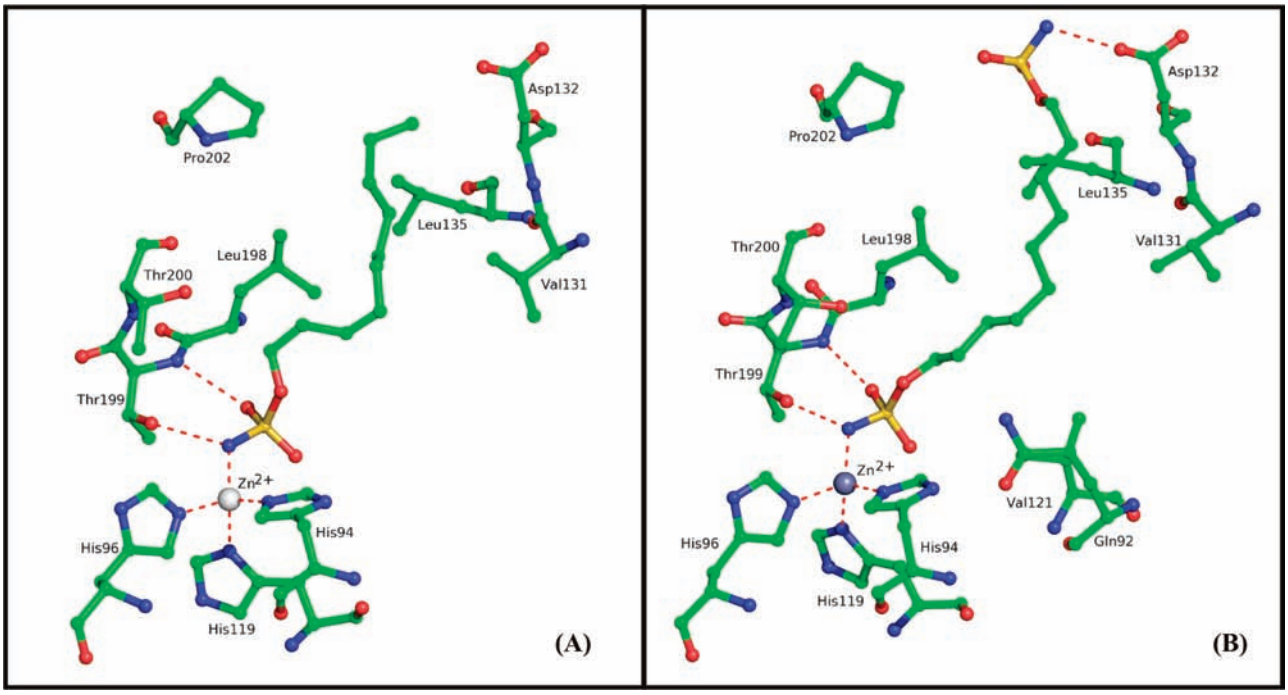

Figure 4. Active site region in the hCA IX−**2** (**A**) and hCA IX−**4** (**B**) complexes showing the residues participating in recognition of the inhibitor molecules. Hydrogen bonds, active site Zn^{2+} coordination, and residues establishing strong van der Waals (distance of <4.5 Å) interactions with the inhibitors are also shown.

where a neutral residue is substituted by a negatively charged one, a potential destabilizing effect on its interaction with the inhibitor hydrophobic tail is observed. In contrast, this last mutation determines the higher affinity of compound **4** toward hCA IX. In fact, the second sulfamate group of the inhibitor, which in the adduct with hCA II forms only hydrophobic contacts, in hCA IX is engaged in a hydrogen bond interaction, stable through MD trajectory (occurrence of ~67%), with the aforementioned Asp132 residue (Figure 1D and Figure 4B). This additional hydrogen bond balances the less favorable van der Waals interactions occurring in the hCA IX−**4** complex with respect to the hCA II−**4** adduct and is responsible for the inversion observed in the affinities of compounds **2** and **4** for the two isoforms.

Conclusions

Aliphatic monosulfamates and bis-sulfamates constitute a class of CAIs distinct from those obtained by the tail or ring approaches. We report here the detailed inhibition profile againt all catalytically active mammalian enzymes, CAs I−XIV, the first X-ray structures for four such compounds in adduct with the physiologically dominant isoform II, in addition to molecular modeling studies for the interaction of two such compounds with hCA IX. These compounds were nanomolar inhibitors of only hCAs II, IX, and XII, unlike aromatic/heterocyclic sulfonamides in clinical use that promiscuously inhibit most of the 12 CA isozymes with low nanomolar affinity. Moreover, the bis-sulfamates incorporating 8 or 10 carbon atoms showed higher affinity for the tumor-associated isozyme CA IX compared to hCA II, whereas the opposite was true for the corresponding monosulfamates. This behavior was explained by considering our crystallographic and molecular modeling studies, which identified the region incorporating amino acid residues 130−136 as a "hot spot" to be considered in structure-based drug design of CA IX-selective inhibitors. Indeed, major differences in such amino acid residues present in the tumor-associated isozyme compared to the cytosolic ones were evidenced, as well as different interactions in which the tail of the inhibitors participate, when bound to the active site of these isozymes. Thus, aliphatic sulfamates/bis-sulfamates constitute a very interesting case of CAIs leading to isoform-selective compounds, whereas the explanation of their interaction with the enzyme active site furnishes new insight for obtaining compounds with increased affinity and selectivity for the various isozymes.

Experimental Section

Materials. Sulfamates **1**−**4** were prepared as reported earlier,[3−5] whereas other compounds and buffers were from Sigma-Aldrich, Milan, Italy. The 12 CA isozymes used in the experiments were recombinant ones obtained and purified as reported earlier by this group.[14,15]

CA Inhibition Assay. An Applied Photophysics (Oxford, U.K.) stopped-flow instrument has been used for assaying the CA catalyzed CO_2 hydration activity. Phenol red (at a concentration of 0.2 mM) has been used as indicator, working at the absorbance maximum of 557 nm, with 10 mM Hepes (pH 7.5) as buffer and 0.1 M Na_2SO_4 (for maintaining constant the ionic strength), following the CA-catalyzed CO_2 hydration reaction.[18] The CO_2 concentrations ranged from 1.7 to 17 mM for the determination of the kinetic parameters and inhibition constants. For each inhibitor at least six traces of the initial 5−10% of the reaction have been used for determining the initial velocity. The uncatalyzed rates were determined in the same manner and subtracted from the total observed rates. Stock solutions of inhibitor (10 mM) were prepared in distilled−deionized water with 10−20% (v/v) DMSO (which is not inhibitory at these concentrations), and dilutions up to 0.01 nM were done thereafter with distilled−deionized water. Inhibitor and enzyme solutions were preincubated together for 15 min at room temperature prior to assay in order to allow for the formation of the E−I complex. The inhibition constants were

obtained by nonlinear least-squares methods using PRISM 3 and represent the mean from at least three different determinations.[18]

Crystallization, Data Collection, and Refinement. The four hCA II−inhibitor complexes were all obtained by adding a 5 M excess of inhibitor to a 10 mg/mL protein solution in 100 mM Tris-HCl, pH 8.5. Crystals of the complexes were grown using the hanging drop vapor diffusion technique at 293 K. In particular 2 μL of complex solution and 2 μL of precipitant buffer (2.5 M $(NH_4)_2SO_4$, 0.3 M NaCl, 100 mM Tris-HCl (pH 8.2), and 5 mM 4-(hydroxymercurybenzoate)) were mixed and suspended over a reservoir containing 1 mL of precipitant solution. Crystals appeared within 3 days. Prior to cryogenic freezing, the crystals were transferred to the precipitant solution with the addition of 15% (v/v) glycerol. X-ray diffraction data were collected at 100 K at the synchrotron source Elettra in Trieste, Italy, using a Mar CCD detector. Data were integrated and reduced using the *hkl* crystallographic data reduction package (Denzo/Scalepack).[24] Diffraction data for each crystal were indexed in the $P2_1$ space group with one molecule in the asymmetric unit. Unit cell parameters and data reduction statistics are recorded in Table 2. The atomic coordinates of CA II refined at 2.0 Å resolution (PDB entry 1CA2)[22] were used as a starting model for crystallographic refinement after deletion of non-protein atoms. An initial round of rigid body refinement followed by simulated annealing and individual *B* factor refinement was performed using the program CNS.[25] Model visualization and rebuilding was performed using the program O.[26] Inhibitor molecules were identified from peaks in $|F_o| - |F_c|$ maps and were gradually built into the models over several rounds of refinement; restraints on inhibitor bond angles and distances were taken from similar structures in the Cambridge Structural Database,[27] and standard restraints were used on protein bond angles and distances throughout refinement. Water molecules were built into peaks of $>3\sigma$ in $|F_o| - |F_c|$ maps that demonstrated appropriate hydrogen-bonding geometry. The correctness of stereochemistry of the final model was checked using PROCHECK.[28] Final refinement statistics for all structures of hCA II−inhibitor complexes are presented in Table 2.

Modeling Studies and Molecular Dynamics Simulations. The model of the hCA IX catalytic domain (Gly12-Phe260) was built using a procedure previously described by Alterio et al.[14a] Briefly, the hCA IX sequence was retrieved by the Swiss-Prot/TrEMBL[29] database [primary accession number Q16790] and modeled using both hCA II[22] (34% sequence identity) and mCA XIV (44% sequence identity) (PDB entry 1RJ6)[30] X-ray structures as templates. The alignment used for model building procedure was the same as that used previously.[14a] Fifty homology models were built with MODELLER, version 6.2,[31] and their quality was assessed by using PROCHECK[28] and 3D-profile[32] module of INSIGHT II (Accelrys Software Inc.). The best model in term of PROCHECK *G*-factor and 3D-profile score was then complexed to inhibitors **2** and **4** by superimposing the heavy atoms from the three catalytic histidines hCA II−**2** and hCA II−**4** structures to the corresponding atoms of hCA IX model. Both experimental and theoretical (hCAIX−**2** and hCAIX−**4**) complexes were completed by addition of all hydrogen atoms and underwent energy minimization with the SANDER module of AMBER9 package,[33] using the PARM99 force field.[34] Atomic charges of both **2** and **4** molecules were obtained with RESP methodology.[35] **2** and **4** conformations, derived from the corresponding hCA II−inhibitor crystal structures, were fully optimized using GAMESS program[36] at the Hartree−Fock level with STO-3G basis set. Single-point calculations on each optimized molecule was performed at the RHF/6-31G* level. The resulting electrostatic potential was thus used for a one-stage single-conformation RESP charge fitting. Partial charges for the three histidines and the zinc ion were those published by Suarez and Merz.[37] To preserve integral charge of the whole system, partial charges of Cα and Hα atoms of zinc-ligand residues and of N and H atoms of inhibitor sulfonamide groups were modified accordingly. A bonded approach between Zn^{2+} ion and its ligands ensured the experimentally observed tetrahedral Zn^{2+} coordination in all complexes during MD simulations. Equilibrium bond distances and angles were taken from hCA II crystal structures. Force constants of 120, 20, and 30 kcal/(mol Å) were used for N(His)-Zn, N(His)-Zn-N(His), and N(His)-Zn-N(sulfamate) bond stretching and angle bending parameters, respectively. All the torsional parameters associated with Zn^{2+}−ligand interactions were set to zero as in Hoops et al.[38] To perform molecular dynamics simulation in solvent, minimized complexes were confined in truncated octahedron boxes (x, y, $z = 80$ Å) filled with TIP3P water molecules and counterions (Na^+/Cl^-) to neutralize the system. The solvated molecules were then energy minimized through 1000 steps with solute atoms restrained to their starting positions using a force constant of 10 kcal mol^{-1} Å^{-1} prior to molecular dynamics (MD) simulations. After this, the molecules were submitted to 90 ps of restrained MD (5 kcal mol^{-1} Å^{-1}) at constant volume, gradually heating to 300 K, followed by 60 ps of restrained MD (5 kcal mol^{-1} Å^{-1}) at constant pressure to adjust system density. Production MD simulations were carried out at 300 K with a constant pressure for 3 ns and a time step of 1.5 fs. Bonds involving hydrogens were constrained using the SHAKE algorithm.[39] Snapshots from production run were saved every 1000 steps and analyzed with the MOLMOL program.[40]

Acknowledgment. This research was financed in part by a grant from the 6th Framework Programme (FP) of the European Union (DeZnIT project) and by a grant from the 7th FP of EU (Metoxia project). We thank the Sincrotrone Trieste C.N.R./Elettra for giving us the opportunity to collect data at the crystallographic beamline.

References

(1) Maren, T. H. Carbonic anhydrase: chemistry, physiology and inhibition. *Physiol. Rev.* **1967**, *47*, 595–781.
(2) (a) Maren, T. H.; Conroy, C. W. A new class of carbonic anhydrase inhibitor. *J. Biol. Chem.* **1993**, *268*, 26233–26239. (b) Håkansson, K.; Liljas, A. The structure of a complex between carbonic anhydrase II and a new inhibitor, trifluoromethane sulfonamide. *FEBS Lett.* **1994**, *350*, 319–322.
(3) Winum, J.-Y.; Vullo, D.; Casini, A.; Montero, J.-L.; Scozzafava, A.; Supuran, C. T. Carbonic anhydrase inhibitors. Inhibition of cytosolic isozymes I and II and transmembrane, tumor-associated isozyme IX with sulfamates including EMATE also acting as steroid sulfatase inhibitors. *J. Med. Chem.* **2003**, *46*, 2197–2204.
(4) Winum, J. -Y.; Vullo, D.; Casini, A.; Montero, J. -L.; Scozzafava, A.; Supuran, C. T. Carbonic anhydrase inhibitors. Inhibition of transmembrane tumor-associated isozyme IX, and cytosolic isozymes I and II with aliphatic sulfamates. *J. Med. Chem.* **2003**, *46*, 5471–5477.
(5) Winum, J.-Y.; Pastorekova, S.; Jakubickova, L.; Montero, J.-L.; Scozzafava, A.; Pastorek, J.; Vullo, D.; Innocenti, A.; Supuran, C. T. Carbonic anhydrase inhibitors: synthesis and inhibition of cytosolic/tumor-associated carbonic anhydrase isozymes I, II and IX with bis-sulfamates. *Bioorg. Med. Chem. Lett.* **2005**, *15*, 579–584.
(6) Supuran, C. T. Carbonic anhydrases: novel therapeutic applications for inhibitors and activators. *Nat. Rev. Drug Discovery* **2008**, *7*, 168–181.
(7) (a) Supuran, C. T. Diuretics: from classical carbonic anhydrase inhibitors to novel applications of the sulfonamides. *Curr. Pharm. Des.* **2008**, *14*, 641–648. (b) Temperini, C.; Cecchi, A.; Scozzafava, A.; Supuran, C. T. Carbonic anhydrase inhibitors. Interaction of indapamide and related diuretics with twelve mammalian isozymes and X-ray crystallographic studies for the indapamide−isozyme II adduct. *Bioorg. Med. Chem. Lett.* **2008**, *18*, 2567–2573. (c) Temperini, C.; Cecchi, A.; Scozzafava, A.; Supuran, C. T. Carbonic anhydrase inhibitors. Sulfonamide diuretics revisited—old leads for new applications? *Org. Biomol. Chem.* **2008**, *6*, 2499–2506.
(8) (a) Supuran, C. T.; Scozzafava, A.; Conway, J. *Carbonic Anhydrase. Its Inhibitors and Activators*; CRC Press: Boca Raton, FL, 2004;

p 1−363. (b) Kohler, K.; Hillebrecht, A.; Schulze Wischeler, J.; Innocenti, A.; Heine, A.; Supuran, C. T.; Klebe, G. Saccharin inhibits carbonic anhydrases: possible explanation for its unpleasant metallic aftertaste. *Angew. Chem., Int. Ed.* **2007**, *46*, 7697–7699.

(9) (a) Pastorekova, S.; Parkkila, S.; Pastorek, J.; Supuran, C. T. Carbonic anhydrases: current state of the art, therapeutic applications and future prospects. *J. Enzyme Inhib. Med. Chem.* **2004**, *19*, 199–229. (b) Supuran, C. T.; Scozzafava, A.; Casini, A. Development of Sulfonamide Carbonic Anhydrase Inhibitors. In *Carbonic Anhydrase. Its Inhibitors and Activators*; Supuran, C. T., Scozzafava, A., Conway, J., Eds.; CRC Press: Boca Raton, FL, 2004; pp 67−147. (c) Thiry, A.; Dogné, J. M.; Masereel, B.; Supuran, C. T. Targeting tumor-associated carbonic anhydrase IX in cancer therapy. *Trends Pharmacol. Sci.* **2006**, *27*, 566–573.

(10) (a) Scozzafava, A.; Mastrolorenzo, A.; Supuran, C. T. Modulation of carbonic anhydrase activity and its applications in therapy. *Expert Opin. Ther. Pat.* **2004**, *14*, 667–702. (b) Winum, J. Y.; Montero, J. L.; Scozzafava, A.; Supuran, C. T. New zinc binding motifs in the design of selective carbonic anhydrase inhibitors. *Mini-Rev. Med. Chem.* **2006**, *6*, 921–936. (c) Supuran, C. T. Carbonic anhydrase inhibitors in the treatment and prophylaxis of obesity. *Expert Opin. Ther. Pat.* **2003**, *13*, 1545–1550.

(11) (a) Krishnamurthy, V. M.; Kaufman, G. K.; Urbach, A. R.; Gitlin, I.; Gudiksen, K. L.; Weibel, D. B.; Whitesides, G. M. Carbonic anhydrase as a model for biophysical and physical−organic studies of proteins and protein−ligand binding. *Chem. Rev.* **2008**, *108*, 946–1051. (b) Stiti, M.; Cecchi, A.; Rami, M.; Abdaoui, M.; Barragan-Montero, V.; Scozzafava, A.; Guari, Y.; Winum, J. Y.; Supuran, C. T. Carbonic anhydrase inhibitor coated gold nanoparticles selectively inhibit the tumor-associated isoform IX over the cytosolic isozymes I and II. *J. Am. Chem. Soc.* **2008**, *130*, 16130–1.

(12) Thiry, A.; Dogné, J. M.; Supuran, C. T.; Masereel, B. Anticonvulsant sulfonamides/sulfamates/sulfamides with carbonic anhydrase inhibitory activity: drug design and mechanism of action. *Curr. Pharm. Des.* **2008**, *14*, 661–671.

(13) (a) Supuran, C. T.; Di Fiore, A.; De Simone, G. Carbonic anhydrase inhibitors as emerging drugs for the treatment of obesity. *Expert Opin. Emerging Drugs* **2008**, *13*, 383–392. (b) De Simone, G.; Di Fiore, A.; Supuran, C. T. Are carbonic anhydrase inhibitors suitable for obtaining antiobesity drugs? *Curr. Pharm. Des.* **2008**, *14*, 655–660.

(14) (a) Alterio, V.; Vitale, R. M.; Monti, S. M.; Pedone, C.; Scozzafava, A.; Cecchi, A.; De Simone, G.; Supuran, C. T. Carbonic anhydrase inhibitors: X-ray and molecular modeling study for the interaction of a fluorescent antitumor sulfonamide with isozyme II and IX. *J. Am. Chem. Soc.* **2006**, *128*, 8329–8335. (b) Dubois, L.; Douma, K.; Supuran, C. T.; Chiu, R. K.; van Zandvoort, M. A. M. J.; Pastorekova, S.; Scozzafava, A.; Wouters, B. G.; Lambin, P. Imaging the hypoxia surrogate marker CA IX requires expression and catalytic activity for binding fluorescent sulfonamide inhibitors. *Radiother. Oncol.* **2007**, *83*, 367–373. (c) D'Ambrosio, K.; Vitale, R. M.; Dogné, J. M.; Masereel, B.; Innocenti, A.; Scozzafava, A.; De Simone, G.; Supuran, C. T. Carbonic anhydrase inhibitors: bioreductive nitro-containing sulfonamides with selectivity for targeting the tumor associated isoforms IX and XII. *J. Med. Chem.* **2008**, *51*, 3230–3237. (d) Thiry, A.; Supuran, C. T.; Masereel, B.; Dogné, J. M. Recent developments of carbonic anhydrase inhibitors as potential anticancer drugs. *J. Med. Chem.* **2008**, *51*, 3051–3056.

(15) Maresca, A.; Temperini, C.; Vu, H.; Pham, N. B.; Poulsen, S. A.; Scozzafava, A.; Quinn, R. J.; Supuran, C. T. Non-zinc mediated inhibition of carbonic anhydrases: coumarins are a new class of suicide inhibitors. *J. Am. Chem. Soc.* **2009**, *131*, 3057–3062.

(16) Alterio, V.; Di Fiore, A.; D'Ambrosio, K.; Supuran, C. T.; De Simone, G. Xray Crystallography of CA Inhibitors and Its Importance in Drug Design. In *Drug Design of Zinc-Enzyme Inhibitors: Functional, Structural, and Disease Applications*; Supuran, C. T., Winum, J. Y., Eds.; Wiley: Hoboken, NJ, 2009; pp 73−138.

(17) (a) Ebbesen, P.; Pettersen, E. O.; Gorr, T. A.; Jobst, G.; Williams, K.; Kienninger, J.; Wenger, R. H.; Pastorekova, S.; Dubois, L.; Lambin, P.; Wouters, B. G.; Supuran, C. T.; Poellinger, L.; Ratcliffe, P.; Kanopka, A.; Gorlach, A.; Gasmann, M.; Harris, A. L.; Maxwell, P.; Scozzafava, A. Taking advantage of tumor cell adaptations to hypoxia for developing new tumor markers and treatment strategies. *J. Enzyme Inhib. Med. Chem.* **2009**, *24* (S1), 1–39. (b) Chiche, J.; Ilc, K.; Laferrière, J.; Trottier, E.; Dayan, F.; Mazure, N. M.; Brahimi-Horn, M. C.; Pouysségur, J. Hypoxia-inducible carbonic anhydrase IX and XII promote tumor cell growth by counteracting acidosis through the regulation of the intracellular pH. *Cancer Res.* **2009**, *69*, 358–368.

(18) Khalifah, R. G. The carbon dioxide hydration activity of carbonic anhydrase. I. Stop-flow kinetic studies on the native human isoenzymes B and C. *J. Biol. Chem.* **1971**, *246*, 2561–2573.

(19) (a) Supuran, C. T.; Scozzafava, A. Carbonic anhydrase inhibitors. *Curr. Med. Chem.: Immunol., Endocr. Metab. Agents* **2001**, *1*, 61–97. (b) Supuran, C. T.; Scozzafava, A.; Casini, A. Carbonic anhydrase inhibitors. *Med. Res. Rev.* **2003**, *23*, 146–189.

(20) (a) Scozzafava, A.; Menabuoni, L.; Mincione, F.; Briganti, F.; Mincione, G.; Supuran, C. T. Carbonic anhydrase inhibitors. Part 74. Synthesis of water-soluble, topically effective, intraocular pressure-lowering aromatic/heterocyclic sulfonamides containing cationic or anionic moieties: is the tail more important than the ring ? *J. Med. Chem.* **1999**, *42*, 2641–2650. (b) Scozzafava, A.; Briganti, F.; Mincione, G.; Menabuoni, L.; Mincione, F.; Supuran, C. T. Carbonic anhydrase inhibitors. Synthesis of water-soluble, amino acyl/dipeptidyl sulfonamides possessing long lasting-intraocular pressure lowering properties via the topical route. *J. Med. Chem.* **1999**, *42*, 3690–3700. (c) Scozzafava, A.; Menabuoni, L.; Mincione, F.; Supuran, C. T. Carbonic anhydrase inhibitors. A general approach for the preparation of water soluble sulfonamides incorporating polyamino-polycarboxylate tails and of their metal complexes possessing long lasting, topical intraocular pressure lowering properties. *J. Med. Chem.* **2002**, *45*, 1466–1476.

(21) Nishimori, I.; Minakuchi, T.; Onishi, S.; Vullo, D.; Cecchi, A; Scozzafava, A.; Supuran, C. T. Carbonic anhydrase inhibitors. Cloning, characterization and inhibition studies of the cytosolic isozyme III with sulfonamides. *Bioorg. Med. Chem.* **2007**, *15*, 7229–7236.

(22) Eriksson, A. E.; Jones, T. A.; Liljas, A. Refined structure of human carbonic anhydrase II at 2.0 Å resolution. *Proteins: Struct. Funct.* **1988**, *4*, 274–282.

(23) Cappalonga Bunn, A. M.; Alexander, R. S.; Christianson, D. W. Mapping protein−peptide affinity: binding of peptidylsulfonamide inhibitors to human carbonic anhydrase II. *J. Am. Chem. Soc.* **1994**, *116*, 5063–5068.

(24) Otwinowski, Z.; Minor, W. Processing of X-ray diffraction data collected in oscillation mode. *Methods Enzymol.* **1997**, *276*, 307–326.

(25) Brunger, A. T.; Adams, P. D.; Clore, G. M.; De Lano, W. L.; Gros, P.; Grosse-Kunstleve, R. W.; Jiang, J. S.; Kuszewski, J.; Nilges, M.; Pannu, N. S.; Read, R. J.; Rice, L. M.; Simonson, T.; Warren, G. L. Crystallography & NMR system: a new software suite for macromolecular structure determination. *Acta Crystallogr., Sect. D* **1998**, *54*, 905–921.

(26) Jones, T. A.; Zou, J. Y.; Cowan, S. W.; Kjeldgaard, M. Improved methods for building protein models in electron density maps and the location of errors in these models. *Acta Crystallogr., Sect. A* **1991**, *47*, 110–119.

(27) Allen, F. H. The Cambridge Structural Database: a quarter of a million crystal structures and rising. *Acta Crystallogr., Sect. B* **2002**, *58*, 380–388.

(28) Laskowski, R. A.; MacArthur, M. W.; Moss, D. S.; Thornton, J. M. PROCHECK, a program to check the stereochemical quality of protein structures. *J. Appl. Crystallogr.* **1993**, *26*, 283–291.

(29) Boeckmann, B.; Bairoch, A.; Apweiler, R.; Blatter, M. C.; Estreicher, A.; Gasteiger, E.; Martin, M. J.; Michoud, K.; O'Donovan, C.; Phan, I.; Pilbout, S.; Schneider, M. The SWISS-PROT protein knowledgebase and its supplement TrEMBL in 2003. *Nucleic Acids Res.* **2003**, *31*, 365–370.

(30) Whittington, D. A.; Grubb, J. H.; Waheed, A.; Shah, G. N.; Sly, W. S.; Christianson, D. W. Expression, assay, and structure of the extracellular domain of murine carbonic anhydrase XIV: implications for selective inhibition of membrane-associated isozymes. *J. Biol. Chem.* **2004**, *279*, 7223–7228.

(31) Sali, A.; Blundell, T. J. Comparative protein modeling by satisfaction of spatial restraints. *J. Mol. Biol.* **1993**, *234*, 779–815.

(32) Bowie, J. U.; Luthy, R.; Eisenberg, D. A method to identify protein sequences that fold into a known three-dimensional structure. *Science* **1991**, *253*, 164–170.

(33) Case, D. A.; Darden, T. A.; Cheatham, T. E., III; Simmerling, C. L.; Wang, J.; Duke, R. E.; Luo, R.; Merz, K. M.; Pearlman, D. A.; Crowley, M.; Walker, R. C.; Zhang, W.; Wang, B.; Hayik, S.; Roitberg, A.; Seabra, G.; Wong, K. F.; Paesani, F.; Wu, X.; Brozell, S.; Tsui, V.; Gohlke, H.; Yang, L.; Tan, C.; Mongan, J.; Hornak, V.; Cui, G.; Beroza, P.; Mathews, D. H.; Schafmeister, C.; Ross, W. S.; Kollman, P. A. *AMBER 9*; University of California: San Francisco, CA, 2006.

(34) Wang, J.; Cieplak, P.; Kollman, P. A. How well does a restrained electrostatic potential (RESP) model perform in calculating conformational energies of organic and biological molecules? *J. Comput. Chem.* **2000**, *21*, 1049–1074.

(35) Bayly, C. I.; Cieplak, P.; Cornell, W. D.; Kollman, P. A. A well-behaved electrostatic potential based method using charge restraints for determining atom-centered charges: the RESP model. *J. Phys. Chem.* **1993**, *97*, 10269–10280.

(36) Schmidt, M. W.; Baldridge, K. K.; Boatz, J. A.; Elbert, S. T.; Gordon, M. S.; Jensen, J. J.; Koseki, S.; Matsunaga, N.; Nguyen, K. A.; Su, S.; Windus, T. L.; Dupuis, M.; Montgomery, J. A. General atomic and molecular electronic structure system. *J. Comput. Chem.* **1993**, *14*, 1347–1363.
(37) Suarez, D.; Merz, K. M., Jr. Molecular dynamics simulations of the mononuclear zinc-b-lactamase from *Bacillus cereus*. *J. Am. Chem. Soc.* **2001**, *123*, 3759–3770.
(38) Hoops, S. C.; Anderson, K. W.; Merz, K. M., Jr. Force field design for metalloproteins. *J. Am. Chem. Soc.* **1991**, *113*, 8262–8270.
(39) Ryckaert, J.-P.; Ciccotti, G.; Berendsen, H. J. C. Numerical integration of the Cartesian equations of motion of a system with constraints: molecular dynamics of *n*-alkanes. *J. Comput. Phys.* **1997**, *23*, 327–341.
(40) Koradi, R.; Billeter, M.; Wuthrich, K. MOLMOL: a program for display and analysis of macromolecular structures. *J. Mol. Graphics* **1996**, *14*, 51–55.